LATERAL STABILITY AND SIDE SLIP OF THE VEHICLE WITH KINETIC STORAGE SYSTEM (KESS)

Venelin Stoyanov Jivkov

Department Theory of Mechanisms and Machines, Technical University of Sofia, 8, Kl. Ochridski Blvd, 1000 Sofia, Bulgaria,
e-mail: jivkov@tu-sofia.bg

Abstract. This paper investigate the influence of kinetic energy battery on the behavior of the car in a turn, overtaking another vehicle, overcoming bumps in the road at a constant speed stability and natural frequencies. The dynamic model of the car is flat, as the axis of the super flywheel coincides with car's longitudinal one. The case of a stationary connection of the kinetic energy system to the car frame was mainly considered and subsequently the influence of its elastic suspension with two add relative degrees of freedom was analyzed. The frequency spectrum, the conditions for stability of the movement and integral characteristics of the transient processes for lateral wheel slip of the tires were calculated. The systems of linear differential equations with variable coefficients were sold by the T-transformation Method, i.e. by means of a short Taylor series in which the end of each serving as the beginning of the next. Numerous examples are numerically solved and demonstrated.

Keywords: t-transformation, tailor series transient processes, natural frequency and stability, lateral slip.

1. INTRODUCTION

In the middle of the last century, the idea arose of using the energy when stopping the vehicle by accumulating it in high-speed flywheels, later called super flywheels, and then using it in process of car's accelerating and motion.

One of the first apologist was Prof. D. Rabenhorst from John Hopkins University – USA, who created research Laboratory whose main activity was investigating the application possibilities of super flywheels in industry (UPS, Tokamak, Railway Sub- stations etc.) and transport equipment (additional energy sources] [1]).

With the development of science and technology, the creation of high-strength materials (Composites, Kevlar, Quartz and Carbon threads etc.),

DOI: 10.7546/EngSci.LIX.24.04.04

with relatively low mass density, as well as precise high-speed bearing assemblies, preserved vacuum etc. the angular speeds of super flywheels reached (6–7).10^3 [1/s].

The first engineering's practical application in transport technics was the Swiss "Gyrobus" with large monolithic low-speed flywheel (with diameter of about 2.5 meters).

This transport's innovation was able to move independently between two energy charging stations at only about 800 meters.

Modern super fly wheels are now usually wound by pre-stressed treads with polymer filling with large kinetic moment $J\Omega$, which affects the behavior of the vehicle.

The use of the kinetic accumulators is most effective in successively alternating transient modes, is there are set of start/stop modes or in another words, if the means of transport works in the conditions of the big city.

In recent years kinetic energy systems (KES) found application as additional energy sources in combinations with internal combustion engines (ICE) or electric motors [2], [3], [4], [5]. These hybrid systems are already found in formula one cars [6], in some luxury automobiles [7] and in city's omnibuses and etc.

Partly, the influence of the kinetic moment of the super flywheel on the behavior of the vehicle is investigated in [8] and [9], proving that the vertical position of the axis of the flywheel relative to the road's plane is preferable.

In the present study, the influence of the $J\Omega$ of the kinetic battery on the controllability, stability, frequency spectrum, lateral elastic drift of the automobile's tires in the conditions of turning and overtaking, with the (not so good) longitudinal arrangement of the battery with respect to it's frame, was analytical analyzed in two cases – a fixed and elastically suspended.

2. THEORETICAL CONSIDERATION

Fig. 1 shows the kinematic scheme of a vehicle with a kinetic energy accumulator in conditions of a turn with constant radius and speed of movement, overtaking and kinematic disturbance from the side of the road. To shorten the computational procedures without significantly reducing the community, a planar dynamical model was chosen [8], [9]. Theoretically, two cases have been considered, the first one with the power unit fixedly connected to the frame of the car and the second one – with suspended one.

To study the influence of the super flywheel's kinetic moment – $J\Omega$ on the behavior of the vehicle, the relatively unfavorable orientation of its axis, coinciding with its longitudinal axis was chosen [10]. For obvious reasons, the vehicles used in engineering practice [11], [12] with similar energy units have axes normal to the road plane.

The selected generalized coordinates are: φ [–] – rotation of the velocity vector of the car's mass center; ψ [–] – rotation of its frame relative to an axis normal to the road plane and passing through its mass center; Φ [–] rotation (galloping) relative to an axis perpendicular to the first.

In Fig. 1 – P is momentary center of rotation of the car; R [m] is the radius of the turn; Z_1 and Z_2 [N] are elastic reactions of the tires in the road plane.

2.1. Immovable connected energy unit with the car's frame

2.1.1. Notation and basic dependencies

$l_1 = \vec{AS}$; $l_2 = \bar{B}S$; $l_3 = \bar{W}S$; [m]
δ – lateral wheel slip of the car's mass center [–]
S – mass center of the car [–]
W – aerodynamic center [–]
J [kgm^2]; $J\Omega$ [kgm^{2}s^{-1}] – mass inertial and kinetic moments of the super flywheel
Y_1 – side wind force [N]
Z_1 and Z_2 – side elastic reactions of the tires [N]
c_1 and c_2 – side elastic coefficients [N]
λ_1 – natural frequency [1/s]
m – mass of the vehicle [kg]
$h.\sin\omega t$ – harmonic excitation from the road [m]
qt – slope of the road [-]
n – dissipation in the suspension [1/s]
ρ – natural frequency of the suspension [1/s^2]
α – control signal of the turning [–]
$\delta = \psi - \varphi$ [–]
θ_z and θ_η – mass moments of inertia of the car [kgm^2]
V_A and V_B velocities of the first and second wheels [m/s].

All numerical calculations in the present study were performed with the following physical –geometrical parameters of the mechanical system:
$c_1 = c_2 = 1.04E5$ [N/rad]; $l_1 = 1.2$ [m]; $l_2 = 1.5$ m $= 1575$ [kg]
$\theta_z = 2.9E3$; $\theta_\eta = 3E3$ [kgm^2]; $n = 0.39$ [1/s]; $\rho = 3.75$ [1/s^2]
$h = 0.1$ [m]; $V = (22.5 - 44.5)$ [m/s]; $\alpha = 0.01$ [–]; $\omega = 12.5$ [1/s]
$J\Omega = (2 - 12)E3$ [kgm^2/s]; $q = 9$ [12/s];

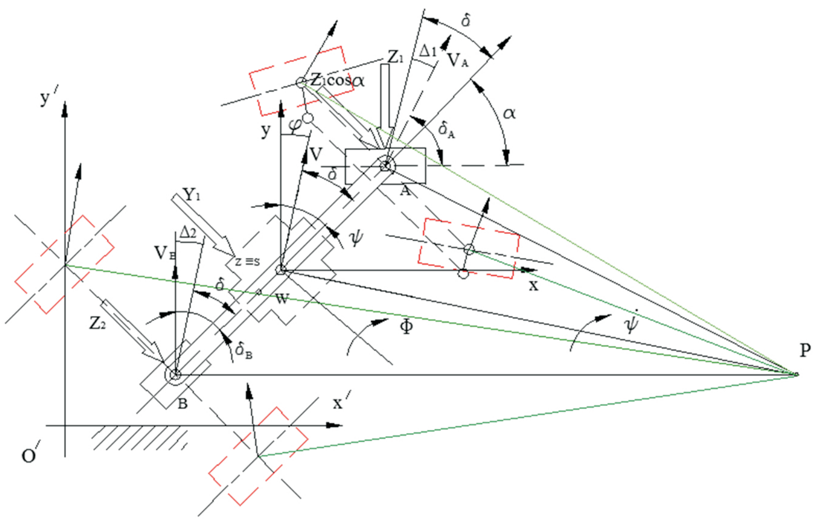

a)

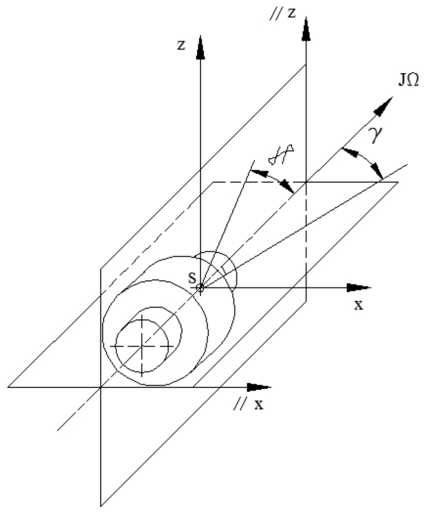

b)

Fig. 1. Kinematic scheme of the vehicle in the turn

2.1.2. Equations of motion

The dynamic equilibrium of the car in the corner is described by an equality of the acted forces in the plane of the road and two such moments with respect to the both axes [13], [14], [15], [16].

$$\begin{aligned} &mV\dot{\varphi} = Z_2 + Z_1 \cos\alpha + Y_1 \\ &\theta_z \ddot{\psi} = l_1 Z_1 \cos\alpha - Z_2 l_2 \pm J\Omega\dot{\Phi} - Y_1 l_3 \\ &\ddot{\Phi} = -n\dot{\Phi} - \rho\Phi \mp \frac{J\Omega\dot{\psi}}{\theta_\eta} = h\sin\omega t + qt, \end{aligned} \tag{1}$$

where

$$\begin{aligned} &Z_1 = c_1\delta_A = c_1(\alpha + \delta - \Delta_1) = c_1\left(\alpha + \delta - \frac{l_1\dot{\psi}}{V}\right) \\ &Z_2 = c_2\delta_B = c_2(\delta + \Delta_2) = c_2\left(\delta + \frac{l_2\dot{\psi}}{V}\right) \end{aligned} \tag{2}$$

$$mV\dot{\varphi} = \frac{mV^2}{R}; \quad \delta = \psi - \varphi.$$

Lets assume that

$$X_1 = \varphi;\ X_2 = \psi;\ X_3 = d\psi/dt;\ X_4 = \Phi;\ X_5 = d\Phi/dt. \tag{3}$$

With these assumptions, the system of equations (1) is transformed in to the following system of five differential equations of the first order with variable coefficients.

$$\begin{aligned} \frac{dX_1}{dt} &= (a_1 + a_2\cos\alpha)X_2 - (a_1 + a_2\cos\alpha)X_1 \\ &\quad +(a_3 - a_4\cos\alpha)X_3 + a_2\alpha\cos\alpha + y_1 \\ \frac{dX_2}{dt} &= X_3 \\ \frac{dX_3}{dt} &= -(a_1 + a_2\cos\alpha)X_2 - (a_1 + a_2\cos\alpha)X_1 \\ &\quad -(a_3 + a_4\cos\alpha)X_3 \pm b_1X_5 + a_2\alpha\cos\alpha + y_2 \\ \frac{dX_4}{dt} &= X_5 \\ \frac{dX_5}{dt} &= -nX_5 - \rho X_4 \pm b_2X_3 + h\sin\omega t + qt \end{aligned} \tag{4}$$

by next initial condition

$$t = 0;\ \ngtr X_1 = X_{10};\ X_2 = X_{20};\ X_3 = X_{30};\ X_4 = X_{40};\ X_5 = X_{50} \quad (5)$$

where

$$\begin{aligned} &a_1 = c_2/mV; \quad a_2 = c_1/mV; \quad a_3 = c_2 l_2/mV^2; \quad a_4 = c_1 l_1/mV^2 \\ &d_1 = c_2 l_2/\theta_z; \quad d_2 = c_1 l_1/\theta_z; \quad d_3 = c_2 l_2^2/\theta_z V; \quad d_4 = c_1 l_1^2/\theta_z \\ &b_1 = J\Omega/\theta_z; \quad b_2 = J\Omega/\theta_\eta; \quad y_1 = Y_1/mV; \quad y_2 = Y_1 l_3/\theta_z \end{aligned} \quad (6)$$

The influence of the kinetic moment JΩ of the energy unit on the lateral elastic slip (draft) of the car/s tires under deterministic signal on the driver side is investigated in the space of the parameters of the mechanical system for the following control effects:

- a turn with constant radius R and speed V $\alpha = \text{const.}$: $\alpha^*(0) = \infty$
- overtaking another vehicle $\alpha = \propto (t)$
- movement on a strait section and harmonic disturbing from the road $f(t) = h.\sin\omega t$.

2.1.3. Natural frequencies

For $t = 0$, $\alpha = \text{const}$ and $\alpha* = \infty$ the frequency equation, corresponding to a (4) homogeneous system differential equations has the form (Jante 1963[21]), (Patas et al. 1967[22])

$$\begin{aligned} &\lambda[\lambda^4 + (G + n + A)\lambda^3 + (Gn + \rho + b_1 b_{2+} GA + An + D - DF)\lambda^2 \\ &\quad + (\rho G + AGn + A\rho + Ab_1 b_2 + Dn - DFn)\lambda \\ &\quad + (AG\rho + D\rho - DF\rho)] > 0 \end{aligned} \quad (7)$$

where $A = a_1 + a_2 \cos\alpha$; $F = a_1 - a_4 \cos\alpha$; $D = d_1 - d_2 \cos\alpha$; $G = d_3 + d_4 \cos\alpha$.

The frequency spectrum consists of three real frequencies, one of which is equal to zero and two imaginary ones. Fig. 2 and Fig. 3 shows the graphs of the real λ^* and imaginary λ as a function of $J\Omega$ of the super flywheel at the vehicle speed parameters $V = 22.5$, 30 and 44.5 [m/s] numerically calculated by Newton's method (Forsyth 1970)

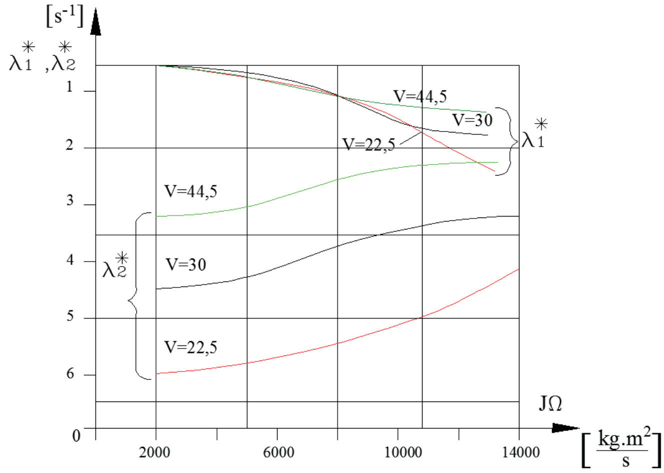

Fig. 2. Real natural frequencies

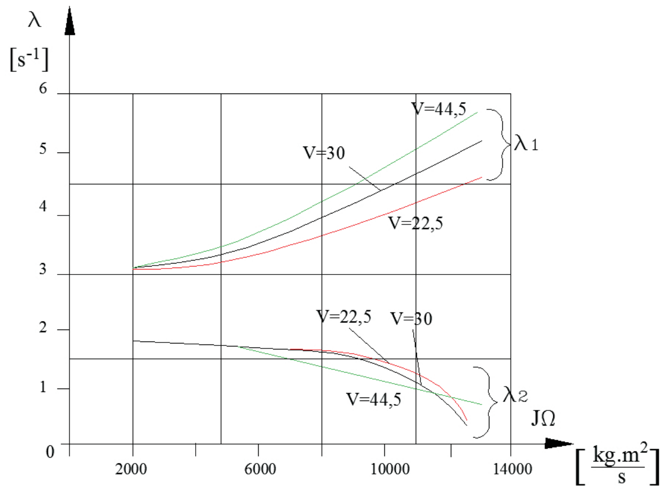

Fig. 3. Imaginary frequencies

2.1.4. Stability of the movement

The stability of the controllability of the vehicle in the conditions of a turn with constant radius and speed of movement is established by applying the the Raus-Hurvitz criteria [17]), [18] for the frequency equation (7), which in this case lead to the following inequalities

$$
\begin{aligned}
&(G+n+A)>0;(Gn+\rho+b_1b_2+GA+An+D+DF)>0\\
&(\rho G+AGn+A\rho+Ab_1b_2+Dn-DFn>0;\\
&(AG\rho+\rho D-\rho DF)>0;\\
&(\rho G+AGn+A\rho+Ab_1b_2+Dn-DFn) \qquad (8)\\
&\times[(G+n+A)(Gn+\rho+b_1b_2+GA+An+D+DF)\\
&-(\rho G+AGn+A\rho+Ab_1b_2+Dn-DFn)]\\
&-(AG\rho+D\rho-DF\rho)(G+n+A)^2>0
\end{aligned}
$$

From the analysis of the restrictions (8), their implementation for existing cars is established. The beneficial influence of the kinematic moment $J\Omega$ of the super flywheel through the members b_1 and b_2, which strengthen inequality (8), is noticed [18], [19].

2.1.5. Solutions of the equations

To solve the system of equations (4) in the transient modes of motion under at general control effect from the driver, the method of the T-transformation [20], [21], [22] is applied, which essentially uses short Taylor series for small interval of real time Δt.

Each of arbitrary control action function of the car driver $\alpha =\propto (t)$ can be approximated by

$$\propto= \xi + \upsilon .t \qquad (9)$$

where, ξ and ν are constants suitable defined for each Δt segment

In accordance to T-transformation method, the image of the system of equations (4) is written by

$$X_1(k+1)=\frac{H}{(k+1)}\Bigg\{a_1X_2(k)-a_1X_1(k)+a_3X_3(k)$$

$$+a_2\sum_{l=0}^{k}\frac{(\upsilon H)^l}{l!}X_2(k-l)\cos\left(\frac{nl}{2}+\xi\right)-a_2\sum_{l=0}^{k}\frac{(\upsilon H)^l}{l!}X_1(k-l)\cos\left(\frac{nl}{2}+\xi\right)$$

$$-a_4\sum_{l=0}^{k}\frac{(\upsilon H)^l}{l!}X_3(k-l)\cos\left(\frac{nl}{2}+\xi\right)++a_2\xi\frac{(\upsilon H)^k}{k!}\cos\left(\frac{nk}{k!}+\xi\right)$$

$$+a_2\upsilon\sum_{l=0}^{k}\frac{(\upsilon H)^{(k-l)}}{(k-l)!}\nabla(l-1)\cos\left[\frac{n(k-l)}{2}+\xi\right]+y_1\nabla(k)\Bigg\};$$

$$X_2(k+1)=\frac{H}{(k+1)}X_3(k); \tag{10}$$

$$X_3(k+1)=\frac{H}{(k+1)}\Bigg\{-d_1X_2(k)+d_1X_1(k)-d_3X_3(k)\pm b_1X_5(k)$$

$$+d_2\sum_{l=0}^{k}\frac{(\upsilon H)^l}{l!}X_2(k-l)\cos\left(\frac{nl}{2}+\xi\right)-d_2\sum_{l=0!}^{k}\frac{(\upsilon H)^l}{l!}X_1(k-l)\cos\left(\frac{nl}{2}+\xi\right)$$

$$-d_4\sum\frac{(\upsilon H)^l}{l!}X_3(k-l)\cos\left(\frac{nl}{2}+\xi\right)++d_2\xi\frac{(\upsilon H)^k}{k!}\cos\left(\frac{nk}{2}+\xi\right)$$

$$+d_2\upsilon\sum_{l=0}^{k}\frac{(\upsilon H)^{(k-l)}}{(k-l)!}X_3(l-1)\cos\left(\frac{n(k-l)}{2}+\xi\right)+y_1\nabla(k)\Bigg\};$$

$$X_4(k+1)=\frac{H}{k+1}X_5(k);$$

$$X_5(k+1)=\frac{H}{k+1}\Bigg[-nX_5(k)-\rho X_4(k)\mp b_2X_3(k)$$

$$+h\frac{(\upsilon H)^k}{k!}\sin\left(\frac{nk}{2}+\xi\right)+q\nabla(k-1)\Bigg],$$

where H is a constant scale of time

The solution of each generalized coordinate is found in the form

$$\frac{dX_i(t)}{dt}\ \dot{\rightleftarrows}\ \frac{k+1}{H}X_i(k+1);\ X(t)_i=\sum_{k=0}^{\infty}X_i(k)\left(\frac{t}{H}\right)^k;\ (i=1,2,3,4,5)$$

$$X_i(t)\ \dot{\rightleftarrows}\ X_i(k)=\frac{H^k}{k!}\left[\frac{9^kX_i(t)}{9^{tk}}\right]_{t=0}\ \text{for } k\geq 0 \text{ and } =0,\ k\lhd 0; \tag{11}$$

where the functions, represented by (9) are

$$\cos(\upsilon t+c)\doteq\frac{(\upsilon H)^k}{k!}\cos(\frac{nk}{2}+\xi);$$

$$X_i\cos(\upsilon t+\xi)\doteq\sum_{l=0}^{k}\frac{(\upsilon H)^l}{l!}X_i(k-l)\cos\left(\frac{nl}{2}+\xi\right);$$

$$t\cos(\upsilon t+\xi)\doteq\sum_{l=0}^{k}H\frac{(\upsilon H)^{(k-l)}}{(k-l)!}\nabla(l-1)\cos\left[\frac{n(k-l)}{2}+\xi\right], \tag{12}$$

respectively

$$\begin{aligned}&\nabla(k-1)=1\rightarrow k=1;=0\rightarrow k\neq 1;\\&\nabla(k)=1\rightarrow k=0;=0\rightarrow k\neq 0;X_i(0)=X_i^0.\end{aligned} \tag{13}$$

After setting $\mathbf{k}\ =0\infty$ and subsequently substitution in (10) is obtained in the process for which the solution (11) is sought for the interval from 0 to H.

According to the already known values of X_i (1,2,3.4,5), the solution can be continued.

The number of terms of the series Taylor series approximates the function with predetermined permissible error in the corresponding time interval from 0 to H.

$$X_i(t)=\sum_{k-0}^{\infty}X_i(k)\left(\frac{t}{H_1}\right)^k;\quad t=(0-H)\text{ and etc.} \tag{14}$$

The time duration of the transient process for which the solution is sought is divided into a finite number of intervals, and in each interval the function is represented by Taylor series that converge quickly.

The first few terms of the corresponding (10) series are written by

$K=0$

$$\begin{aligned}X_1(1)&=H[a_1X_2^0-a_1X_1^0+a_3X_3^0+a_2X_2^0\cos(\xi)-a_2X_1^0\cos(\xi)\\&\qquad-a_4X_3^0\cos(\xi)+a_2\xi\cos(\xi)]\\X_2(1)&=HX_3^0\\X_3(1)&=H[-d_1X_2^0+d_1X_1^0+a_3X_3^0\pm b_1X_5^0+d_2X_1^0\cos(\xi)\\&\qquad-d_4X_3^0\cos(\xi)+d_2\xi\cos(\xi)]\\X_4(1)&=HX_5\\X_5(1)&=H[-nX_5^0-pX_4^0\mp b_2X_3^0+H\sin(\xi)]\end{aligned}$$

$$K = 1 \tag{15}$$

$$X_1(2) = \frac{H}{2}\Bigg[a_1X_2^1 - a_1X_1^1 + a_3X_3^1 + a_2R_1 - a_4R_3$$
$$+ a_2\xi\frac{(\upsilon H)}{1}\cos\left(\frac{n}{2}+\xi\right) + a_2\upsilon H\cos(\xi)\Bigg];$$
$$X_2(2) = \frac{H}{2}X_3^1;$$
$$X_3(2) = \frac{H}{2}\Bigg[- d_1X_2^1 + d_1X_1^1 - d_3X_3^1 \pm b_1X_5^1 + R_1d_2 - R_2d_2 - R_3d_4$$
$$+ d_2\xi\frac{(\upsilon H)}{1}\cos\left(\frac{n}{2}+\xi\right) + d_2\upsilon H\cos(\xi)\Bigg];$$
$$X_4(2) = \frac{H}{2}X_5^1;$$
$$X_5(2) = \frac{H}{2}\left[- nX_5^1 - \rho X_4^1 \mp b_2X_3^1 + h(\frac{wH}{2})\sin\left(\frac{n}{2}+\xi\right)\right].$$

where

$$X_1^1 = X_1(1);\ X_2^1 = X_2(1);\ X_3^1 = X_3(1);\ X_4^1 = X_4(1);\ X_5^1 = X_5(1);$$
$$R_1 = X_2^1\cos(\xi) + X_2^0\frac{(\upsilon H)}{1}\cos\left(\frac{n}{2}+\xi\right);$$
$$R_2 = X_1^1\cos(\xi) + X_1^0\frac{(\upsilon H)}{1}\cos\left(\frac{n}{2}+\xi\right);$$
$$R_3 = X_3^1\cos(\xi) + X_3^0\frac{(\upsilon H)}{1}\cos\left(\frac{n}{2}+\xi\right).$$

$k = 2$ where

$$X_1(3) = \frac{H}{3}\Bigg[a_1X_2^2 - a_1X_1^2 + a_3X_3^2 + a_2S_1 - a_2S_2 - a_4S_3$$
$$+a_2\xi\frac{(\upsilon H)^2}{2}\cos(n+\xi) + a_2(\upsilon H)^2\cos(\frac{n}{2}+\xi)\Bigg];$$
$$X_2(3) = \frac{H}{3}X_3^2;$$
$$X_3(3) = \frac{H}{3}\Bigg[- d_1X_2^2 + d_1X_1^2 - d_3X_3^2 \pm b_1X_5^2 + d_2S_1 - d_2S_2 - d_4S_3$$

$$+d_2\xi\frac{(\upsilon H)^2}{2}\cos(n+\xi)+d_2(\upsilon H)^2\cos(n+\xi)\Bigg];$$

$$X_4(3) = \frac{H}{3}X_5^2;$$

$$X_5(3) = \frac{H}{3}\left[-nX_5^2-\rho X_4^2\mp b_2X_3^2+h\frac{(wH)^2}{2}\sin(n+\xi)\right].$$

where

$$X_1^2=X_1(\xi);\ X_2^2=X_2(2);\ X_3^2=X_3(2);\ X_4^2=X_4(2);\ X_5^2=X_5(2)$$

$$S_1=X_2^2\cos(\xi)+X_2^1\frac{\nu H}{1}\cos\left(\frac{\pi}{2}+\xi\right)+X_2^0\frac{(\nu H)^2}{2}\cos(\pi+\xi)$$

$$S_2=X_1^2\cos(\xi)+X_1^1\frac{\nu H}{1}\cos\left(\frac{\pi}{2}+\xi\right)+X_1^0\frac{(\nu H)^2}{2}\cos(\pi+\xi)$$

$$S_3=X_3^2\cos(\xi)+X_3^1\frac{\nu H}{1}\cos\left(\frac{\pi}{2}+\xi\right)+X_3^0\frac{(\nu H)^2}{2}\cos(\pi+\xi)$$

and etc.

In the process of researching the considered problem, it was found that to achieve higher accuracy, it is necessary to work with the first six terms.

2.2. Elastically suspended kinetic energy unit

Fig. 1 b) shows the elastically suspended energy unit with two add degrees of freedom relative to the vehicle frame with generalized coordinates γ and $\wp$ (rotations with the respect to an axis normal to the road and the car's frame).

2.2.1. Equations of motion

Under these assumptions (Lurie 1961), (Jante 1963) the differential equations, which describe the motion of the mechanical system, takes the form

$$\begin{aligned}
&mV\delta^\bullet = Z_2+Z_1\cos\alpha+mV\psi^\bullet\\
&\vartheta_z\psi^{\bullet\bullet}=l_1Z_1\cos-l_2Z_2+c_\gamma\gamma+\beta_\gamma\gamma^\bullet\\
&\Theta_\gamma(\psi^{\bullet\bullet}+\gamma^{\bullet\bullet})+c_\gamma\gamma+\beta_\gamma\gamma^\bullet+J\Omega(\Phi^\bullet+\wp^\bullet)=0\\
&\Phi^{\bullet\bullet}=-n\Phi^\bullet-\rho\Phi+\frac{c_\wp}{\theta_z}\wp+\frac{\beta_\wp}{\theta_z}\wp^\bullet+\frac{h}{\theta_z}\sin\omega t\\
&\Theta_\wp(\Phi^{\bullet\bullet}+\wp^{\bullet\bullet})+c_\wp\wp+\beta_\wp\wp^\bullet-J\Omega(\psi^\bullet+\gamma^\bullet)=0.
\end{aligned}\tag{16}$$

Additional notations
where

γ and $\wp$ angular coordinates	[–]
c_γ and $c_\wp$ angular stiffness coefficients	[Nm]
β_γ and $\beta_\wp$ angular damping coefficients	[Nms]
Θ_γ and $\Theta_\wp$ mass moments of inertia of the kinetic energy unit	[kgm^2]

If we subtract the expression $mV\Psi^*$ from both sides of the first equation of (16) a direct equation with respect to the δ is obtained, in which the order of the system of differential equations is lowered

$$mV\delta^\bullet = -c_2\left(\delta + \frac{l_2\psi^\bullet}{V}\right) - c_1\left(\alpha + \delta - \frac{l_1\psi^\bullet}{V}\right)\cos\alpha + mV\psi^\bullet \qquad (17)$$

After introducing the next designations

$$X_1 = \delta; X_2 = \psi^\bullet; X_3 = \gamma; X_4 = \gamma^\bullet; X_5 = \Phi; X_6 = \Phi^\bullet; X_7 = \wp; X_8 = \wp^\bullet \quad (18)$$

a system of eight linear equations with variable coefficients of first order similar to (4) is obtained.

Additional physical parameters of the new mechanical system are equal to:

$$\Theta_\gamma = \Theta_\wp = 15 \text{ [kgm}^2\text{]};\ c_\gamma = c_\wp = 15E3 \text{ [Nm]};\ \beta_\gamma = \beta_\wp = 1E2 \text{ [Nms]}.$$

Applying the methodology outlined above, the system of equations (16) is solved again by the T-transform method obtaining expressions similar to (11) for transient processes for lateral wheel slip of the tires and forces in the bearing assembly.

In both cases, a stationary fixed and elastically suspended kinetic energy unit to the frame of the car, the systems of differential equations (3) and (16) are solved numerically under zero initial conditions.

3. NUMERICAL SOLUTIONS

Numerical calculation of (11) was performed with Euler's implicit method [23], [24], distinguished by a high degree of accuracy and wide area of stability by initial conditions $\alpha(0) = \text{const.}$ [–] $\alpha^*(0) = \infty$ [1/s].

Fig. 4 and Fig. 5 show the graphs of the solutions from transient processes – (11) for the lateral elastic drift of the tires of a car in the conditions of a turn with constant radius (R = constant) with control signal $\alpha(0) = 0.2$ [–] and $\alpha^*(0) = \infty$ [1/s] at different kinetic moments $J\Omega$] kgm^2/s] and damping coefficients n [1/s].

The two figures clearly show the influence of the kinetic moment of the super flywheel on the δ [–] of the mass center of the vehicle during the turn. To emphasize the influence of $J\Omega$, the cases with their zero value are also presented, i.e. in the absence of kinetic energy accumulator.

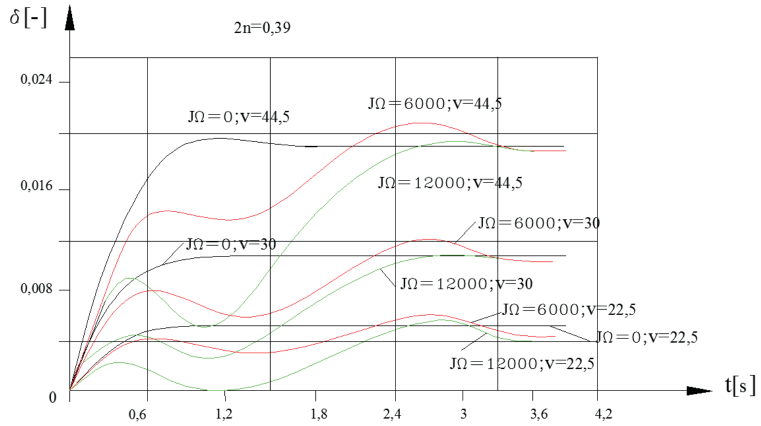

Fig. 4. Transition process of δ at small dissipation coefficient

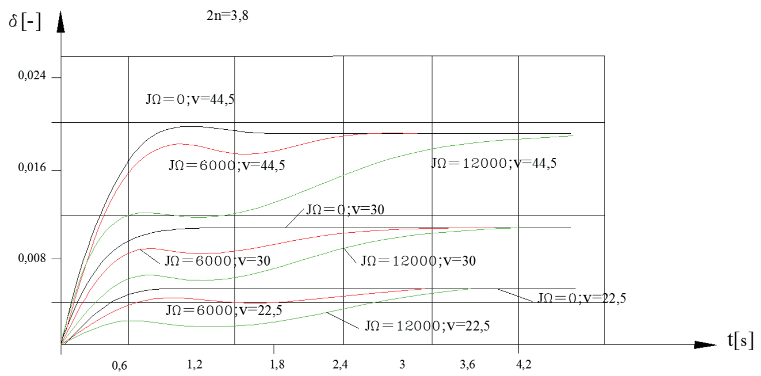

Fig. 5. Transition process of δ by dissipation coefficient $n = 3.8$ [1/s]

With large dissipation in the suspension of the vehicle, a softening of the transient process is noticed, i.e. reduction of δ and stretching over time without exceeding its values at $J\Omega = 0$.

The same effects are also observed at small values of the dissipation $n = 0.39$ [1/s] – Fig. 4, where the difference consists in the presence of damping vibration with a frequency of the ψ coordinate, with the maximum δ-value increasing by approximately five percent.

Very light can be proof that at $t \to \infty$, steady-state value of the lateral elastic draft (slip) of the car's tires for its mass center does not depend of kinetic moment.

$$\delta_{t-\propto} = f(V, c_1, c_2, m, l_1, l_2, \theta_z)$$

Fig. 6 shows the transient process of δ(t) when overtaking another car.

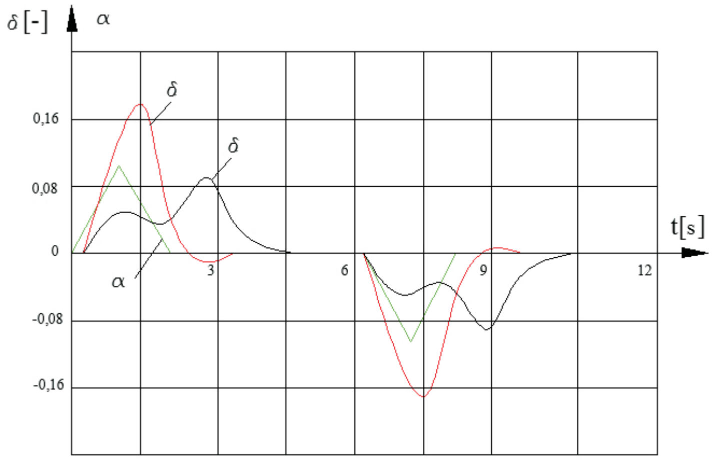

Fig. 6. Transition process at overtaking

The driver's signal in this case is represented by a pace wise linear function at the form:

$$\alpha = \xi + \nu t, \tag{19}$$

where

$$\xi \in 0.1; -0.1; 0, -0.1, \qquad \nu \in 0.1; -0.1, 0, ; -0.1; 0.1,$$

for $J\Omega = 0$ (red line) and $J\Omega = 12$ (black line) [kgm^2/s].

Here again a stretching of the transient process is observed at a more 60% reduction of δ-maximum with the presence of a second wave coping the control signal with phase shift in time requiring correction of the control function.

Fig. 7 depicts the lateral elastic drift of the tires when the car moves along straight section with a kinematic excitation (disturbance) from the road with amplitude h [m] and frequency ω[1/s]. In this case the δ is of order of 2.E-8 [–] from which it follows that JΩ [kgm^2/s] practical does not affect the controllability of the vehicle.

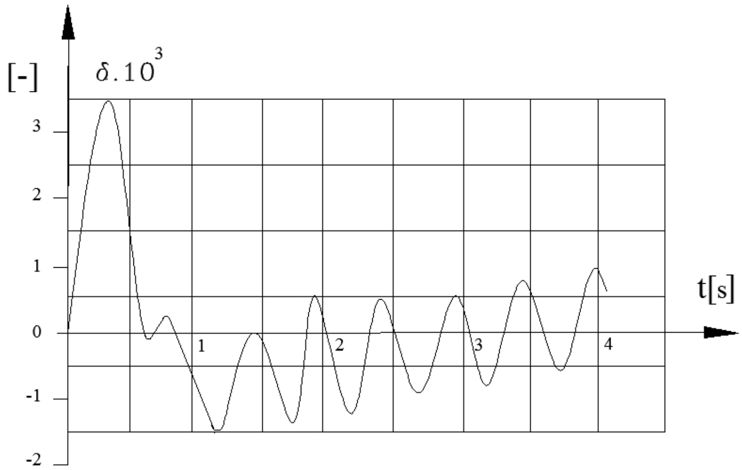

Fig. 7. Kinematic excitation from the road

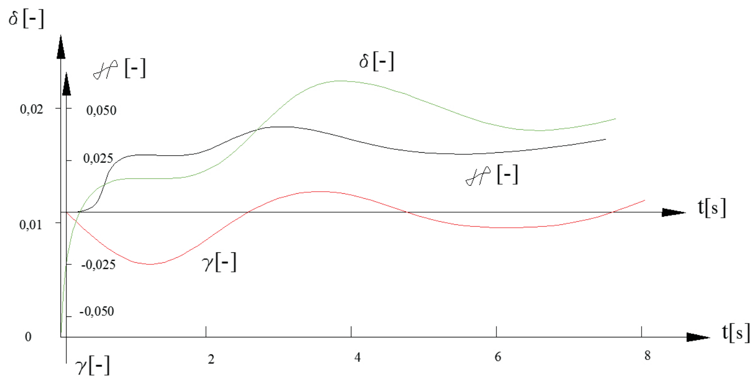

Fig. 8. Elastically suspended unit

For the elastically suspended power unit, Fig. 8 shows the rotations $\gamma[-]$ and $\wp$ $[-]$ relative to the frame of the car, as well as the elastically drift δ $[-]$ – under the same cornering conditions as in the above-mentioned cases.

The graph of the δ $[-]$ is comparable to those of Fig.4 and Fig. 5, and the differences in the ordinates represent the influence of the elastically suspended energy unit.

The essential difference consists in the two-fold stretching of the transient processes for δ $[-]$, as well as the relative rotations γ $[-]$ and $\wp$ $[-]$ in the time. The steady-state values of the delta at t $\to \infty$ are the same as those with fixed connection between the power unit and the body of the vehicle.

The elastically suspension significantly eases the load in the bearing assemblies of the super flywheel when turning, which is clearly evident from Fig. 9(with and without elastically suspension), at 0.2 [m] distance between bearing's support.

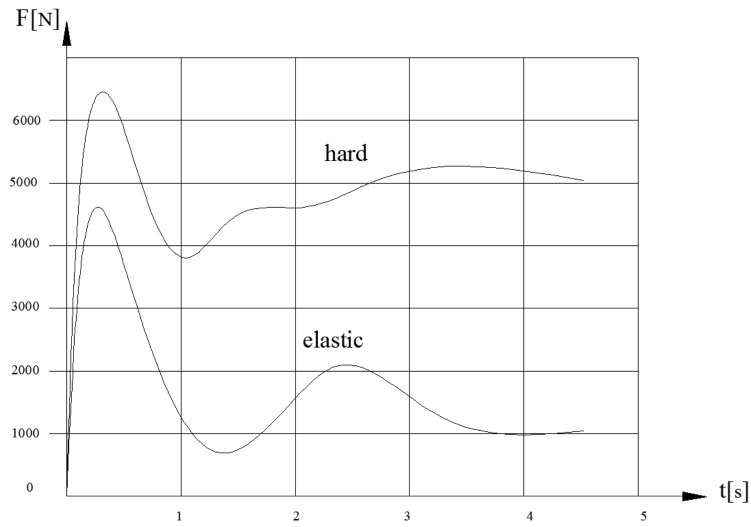

Fig. 9. Power in bearing assembly

4. CONCLUSION

The most important inferences from the theoretical study of the influence of the kinetic moment of the super flywheel on the behavior of the car are:

– The stationary lateral elastic wheel slip of the car's tires $\delta_{t\to\infty}$ does not depend on the magnitude of the kinetic moment of the battery; it depends on the speed, the control signal α and physical- geometrical parameters of the vehicles.
– The transient processes of the elastic drift of the tires to a certain extent worsen the controllability of the car, especially in the conditions of overtaking; for this reason the axis of the super flywheel is vertical to road's plane in the already realized industrial examples.
– Road bumps practically do not affect the controllability of the car's motion.
– Kinetic moment $J\Omega$ have beneficial effect on the stability of the car's motion.
– The elastic suspension of the super flywheel on the frame of the car does not effect the stationary values of the lateral elastic drift of the car's tires, but significantly unloads the bearing assemblies of the kinetic accumulator.

ACKNOWLEDGMENT

This work was supported by the project 11 IF -02-15/03.12.2020 – Kinetic power systems for Industry – Ministry of Economic BG.

REFERENCES

[1] D. Rabenhorst, Primary Energy Storage and the Super-Flywheel, Applied Physics Laboratory, John Hopkins University, TG-1081 (1979).

[2] BRD-Patent 2649241 Omnibus mit Schwungrad Energy Speicher.

[3] F. Hagin, Hydro Und Girospeicher Antriebe Für Stadtomnibuse – MAN Entwicklung (1991).

[4] Ricardo PLC, *Latest News and Updates on Automotive and Energy Innovations*, online: http://www.ricardo.com/en-Gb/News.

[5] FlyBird Systems Team, *Flybird Systems: Advanced Solutions for Energy and Mobility*, online: http://www.flybird.systems.com.

[6] K. Collantine, *The Evolution of KERS in Formula 1: A Game-Changer for 2009*, online: http://f1fanatic.co.uk/2009/01/11/.

[7] Automedia Editorial Team, *Automedia: The Latest Trends and Innovations in the Automotive Industry*, online: http://www.automedia.com.

[8] A. Madhusudhanan, M. Corno, and E. Holweg, Sliding Model-Based Lateral Vehicle Dynamics Control Using Tire Force Measurements, *Vehicle System Dynamics* (2015) **53** (11) 1500–1619, online: https://doi.org/10.1080/00423114.2015.1066018.

[9] V. Jivkov, Behavior of the Car in Turning, *Mechanics of Machines* (1995) **4** 5–10 (in Bulgarian).

[10] M. Guiggani, *The Science of Vehicle Dynamics*, Springer Verlag (2014).

[11] V. Jivkov, *Dynamics and Stability of Vehicle with KERS*, D.Sc. Thesis, Technical University – Sofia (2000) (in Bulgarian).

[12] R. Jassar, *Vehicle Dynamics*, Springer Verlag (2014).

[13] V. Jivkov and V. Draganov, Theoretical Study and Experimental Validation of a Hydrostatic Transmission for a City Bus Hybrid Driveline with Kinetic Energy Storage, *Energies* (2018) **11** (9) 2020–2231, online: https://doi.org/10.3390/en11092200.

[14] V. Jivkov, Steady State Movement of the Car with KERS at Deterministic Sliding of the Rear Bridge, *Mechanics of Machines* (1995) **4** 2–8 (in Bulgarian).

[15] V. Zubov, *Analytical Dynamics of Giro-System*, Leningrad (1961) (in Russian).

[16] A. Lurie, *Analytical Mechanics*, Moscow (1961) (in Russian).

[17] K. Magnus, *The Gyroscope; Theory and Application*, Moscow (1974) (in Russian).

[18] A. Martinuk et al., *Dynamics and Stability of Movement of Transport Vehicles and Machines*, Kiev (1981).

[19] A. PACEJKA, *Tire and Vehicle Dynamics*, 2nd Edition, Elsevier, Butterworth-Heinemann, Berlin-Amsterdam-Tokyo (2006).

[20] G. PUHOV, *Taylor's Transformation Und the Application in the Electro-Technics and Electronics*, Kiev (1978).

[21] A. JANTE, *Die Grundlage der Fahrstabilitet*, Berlin (1963).

[22] K. PATAS, Fahrstabilität und Kurshaltung von Kraftfahrzeugen bei Geradeaus und Kurvenfahrt auf Reale Strasse, *Automobil Industrie* (1967) **4**.

[23] D. FORSYTH, *Machine Methods for Mathematical Calculation*, Moscow, Edition Science (1970) (in Russian).

[24] I. KOZAR, M. PLOVANIC, AND T. SOULOVSKY, Derivation Matrix in Mechanics – Data Approach, *Engineering Review* (2023) **43** (1) 24–25, online: https://doi.org/10.30765/er.1892.

Received November 15, 2024